A Device to Mitigate Vortex Induced Rooftop Suction

David Banks[1], Partha P. Sarkar[2], Fuquiang Wu[3] and Robert N. Meroney[4]

Abstract

Roof failures are often the most common type of wind damage suffered during hurricanes. The device described in this paper offers considerable potential benefit in reducing losses due to roof damage. Schools, shopping malls, industrial sites and residential buildings can make use of this device both as a feature in new designs and as a retrofit enhancement. Results of wind tunnel and full scale tests indicate that peak suction forces are reduced by over 50% near the roof edges. Analysis indicates that this approaches the maximum suction reduction possible for sharp edged roofs.

Introduction

Hurricanes and tropical storms cause some $US 3 billion in property loss annually in the USA. Much of the loss inflicted by such windstorms is water damage to interior contents following a breach of the building's envelope (Cermak 1998). Low-rise buildings typically suffer the most damage (National Research Council 1985), and loss of roof cladding is often the most pervasive type of damage (FEMA 1992).

It is well known that this damage is the result of the extreme suction forces exerted on the building envelope by vortices which form in the separated flow along the edge of low-rise building roofs. As airflow curves over the leading edge of a low-rise building roof, the local flow speed increases, and the pressure drops, causing a negative pressure inside the regions of separated flow. This effect is amplified when a vortex is present; the vortex core houses very low pressures, which are partially transmitted to the roof surface beneath the vortex (Banks and Meroney 2001b).

These vortices can be eliminated by curving or streamlining the roof edge (Richardson and Surry 1994). However, this is often not practicable, for example for buildings with eaves. To retrofit roofs without eaves, a streamlined projection can be added to the wall, though this may need to be somewhat cumbersome to be effective. In lieu of eliminating the straight sharp edges that create the vortices, some studies have examined methods of disrupting the vortices using various roof mounted barriers and screens (Cochran and English 1997; Lin and Surry 1993), and a patent has been issued for a range of devices based on this principle (Kramer and Haage 1975). The barriers in these studies

---

[1] Cermak Peterka Petersen, Inc., 1415 Blue Spruce Drive, Fort Collins, CO 80524, dbanks@cppwind.com.

[2] Wind Simulation and Testing Laboratory, Dept. of AEEM, 2271 Howe Hall (Room 1200), Iowa State University, Ames, IA 50014. ppsarkar@iastate.edu

[3] EQE International, 16850 Diana Lane, Houston, TX 77058. FWu@eqe.com

[4] Wind Engineering and Fluids Laboratory, Engineering Research Center, Colorado State University, Fort Collins, Colorado 80523. meroney@engr.colostate.edu

CEP00-01-1

were mounted near the roof corner, since the conical vortices which form for cornering winds produce the worst suctions of all. This is in part because these vortices are more stable than the cylindrical vortices which form inside the bubble separation for winds normal to a given wall, so that locations near the corner are beneath vortices more consistently than locations away from the corner (see Figure 2 for a simple depiction of the differences between the two flows).

However, the placement of items on the roof to disrupt the vortices presupposes knowledge of the location of the vortex. Studies have shown that the vortices are intermittent and move about on the roof a great deal, both in the case of the conical vortex (Banks et al. 2000; Wu 2000) and the vortices inside the bubble separation (Saathoff and Melbourne 1989). Perhaps as a result, these rooftop obstruction techniques have not proven as effective as those which disrupt the vortices at their source (the sharp roof edge) using devices such as sawtooth parapets or fences (Surry and Lin 1995). The most effective of such devices tested by Surry and Lin, a porous parapet, actually provided a greater reduction in peak suction than even the curved roof corners.

Experiments

Full Scale Tests

This paper also tests a rooftop suction mitigation device which is deployed along the roof's leading edge. This device is designed to disrupt the vortex by deflecting some of the shear layer flow towards the roof inside the separation bubble, and hence is called the flow divider (see Figure 3). The device is intended to be architecturally unobtrusive, and so is relatively small, measuring 100mm (4 inches) in width and sitting 75 mm (3 inches) above the roof surface (Figure 4). It is 13mm (½ inch) thick. The vertical supports were spaced .45m (18 inches) apart.

The device was deployed along the roof edge 3.5m (12 ft) from the instrumented roof corner of the WERFL building, and pictures are provided in Figure 5. This corner featured 25 pressure taps within 3m (10 ft.) of the roof edge, arranged roughly in rows at x = 0.5m, 1.1m, 1.4m, and 2.6m (1.5 ft, 3.6ft, 4.6 ft, and 8.7 ft). The building measures 4m (13 ft.) in height, and has walls of 9.1m and 13.7m (30ft and 45 ft) in length, with an essentially flat roof. The facilities are described in more detail in (Levitan and Mehta 1992).

Tests were conducted over a range of relevant wind directions, encompassing both the conical vortex and bubble separation situations. The flow divider reduced mean and peak suctions at all taps for all vortex producing wind directions. More details of both the experimental configuration and results are provided in (Wu 2000). Figure 6 shows the reduction in suction for tap #50501, which is located at x=1.4m (4.64 ft.) and y=0.35m (1.16ft.).

Model scale tests

The model scale experiments were conducted in the Meteorological boundary layer wind tunnel at CSU using the BII boundary layer as described in (Ham and Bienkiewicz 1998). Because of the small size of the opening between the spoiler and the roof surface, a 1:25 scale model of the TTU WERFL site was used. Pressure tap locations matched those currently in place at the full-scale site, with some additional taps added as indicated in Figure 7. These experiments are described in more detail in (Banks 2000).

It was anticipated that the essentially flat flow divider depicted in Figure 4 will not be suitable for all architectural applications, so two divider shapes were tested, and compared to the porous parapet and a solid parapet. The test configurations are depicted in Fig. 8. Results for the row of taps including tap 50501 are shown in Figure 9. The flat plate was the most effective device.

Several variations on the flat plate were also tested (dimensions below are full scale).

i) 100 mm (4 inch) width, no overhang, angled at 10°
ii) 230 mm (9 inch) width, no overhang, angled at 10°
iii) 230 mm (9 inch) width, 50mm (2 in) overhang, angled at 10°
iv) 230 mm (9 inch) width, 100mm (4 in) overhang, angled at 10°
v) 230 mm (9 inch) width, 50 mm (2 in) overhang, angled at 10°, curved end (see Figure 10a)
vi) 100 mm (4 inch) width, no overhang, angled at -10°

All of these configurations reduced the mean suction considerably, as shown in the area averaged pressure coefficient plots of Figure 11. The results indicated that the overhang provided considerable improvement over the no overhang cases. The downward curvature at the leading edge also appears to provide additional peak suction reduction, though this is not apparent in the mean data. Once again, further information on these tests is available in (Wu 2000).

Finally, Figure 9 confirmed that the presence of a low parapet increase the area of extreme suction by enlarging the roof edge vortices (Bienkiewicz and Sun 1992). The effectiveness of the flow dividing device as a retrofit in such situations was tested by mounting the narrow (100mm full scale) plate on the solid parapet (see Figure 10b). This configuration did reduce suction, but it achieved less than half of the suction reduction possible using the overhanging plate alone.

Discussion: Limits to the potential for suction reduction

As mentioned in the introduction, the vortex acts as a pressure drop amplifier. A fast gust of wind will not only drop the pressure at the point M above the separation region (Figure 1), it will spin the vortex faster, creating a greater suction at the point S. The relationship is expressed by the equation

$$Cp_S(t) = \left(\frac{U_M(t)}{\overline{U}_M}\right)^2 \left(1 - \frac{\overline{U}_M^2}{\overline{U}_{ref}^2}\left[1 + \sin^2(\alpha(t)) \cdot g(t)\right]\right) \tag{1}$$

where U_M is the flow speed at the point M. (This equation is examined in some detail in (Banks and Meroney 2002)). The term $g(t)$ expresses the strength of the vortex. If the vortex has been eliminated, then $g(t) = 0$, and the surface pressure essentially mirrors that at the edge of the separation region:

$$Cp_S(t) = Cp_M(t) = \left(\frac{U_M(t)}{\overline{U}_M}\right)^2 \left(1 - \frac{\overline{U}_M^2}{\overline{U}_{ref}^2}\right) \tag{2}$$

This implies that a measurement of the velocity at the point M will permit a prediction of the lowest possible surface suction. In other words, since U_M is a function of the shape of the building (especially at the roof corner) and of the upstream turbulence, once the vortex is eliminated, Cps could not be further reduced without streamlining the building or interfering with the flow upstream to reduce U_M. Measurements of U_M were made in the CSU wind tunnel, and the behaviour of the calculated Cp_M is compared to that of Cps with and without mitigation in Figure 12. The figure indicates that the suction reduction produced by the flat plate approaches the limit that this theory states is achievable for the WERFL building. Note that the shape of the mean Cp limit in Figure 12a is the result of changes in the mean value of U_M as a function of wind direction (Banks and Meroney 2002). The shape of the limiting probability distribution function (PDF) in Figure 12b is dictated by the turbulence of the flow over the leading edge of the roof. The long, broad negative tail of the PDF for the no mitigation case is the result of the combination of vortex behaviour with local turbulence (Banks and Meroney 2001a).

Conclusions and Recommendations

A relatively small device has been tested which significantly reduces peak suction forces induced by vortices along the edge of roofs. The device is well suited to retrofit buildings with underdesigned roofs that are susceptible to loss of roof cladding in extreme winds.

Considerable additional development of this device is suggested:

1) While the flat plate produced markedly better results than the circular flow deflector, the circular deflector did offer significant suction reduction. It is expected that a large range of shapes (airfoils, rectangles, ovals, and various curves and polygons) could all be tuned to provide performance comparable to that of the flat plate (see Figure 13). This would provide considerable architectural flexibility. Because of the small size of the model scale devices, subtle changes in shape were difficult to assess, and larger scale tests would be needed.

2) It is expected that the device will experience considerable uplift. Some Computational Fluid Dynamic modeling of these force has been performed at CSU, but the results remain as yet unverified experimentally. These loads need to be determined to know when the device can be safely installed; were it to come loose in a storm, the loads on the roof surface would double.

3) The lift force on the device could be used to advantage in its deployment. While the simplest technique is to have the device mounted permanently, it may be desirable for aesthetic or architectural reasons to deploy the device only in the event of a severe storm, much as is the current practice for storm shutters. This can be facilitated by making the device retractable, as illustrated in Figure 14. While it is envisaged that the deployment could be initiated manually, a technique for automated deployment could take advantage of the lift force exerted on the device while it lies flat against the roof surface. Through the use of a spring or other resistance to the wind's lift force, the device would remain retracted by default. It would only be pulled into the correct position to disrupt the vortices in the presence of a sufficiently strong wind. Once deployed, it could optionally lock into place.

4) This device could be deployed not only along the edges of flat roofs, as tested, here, but along the ridge of a gable or hipped roof, and even along the building corners where two walls meet, since flow separation and the attendant wind damage happens at all of these locations. Tests to quantify the suction reduction in these cases could be undertaken.

Acknowledgements

The device was developed and tested while the authors were affiliated with Texas Tech University and at Colorado State University. The work was part of the Cooperative Program in Wind Engineering, which was supported by National Science Foundation grant number CMS-9411147.

References

Banks, D. (2000). "The Suction Induced by Conical Vortices on Low-Rise Buildings with Flat Roofs," Ph.D. dissertation, Colorado State University, Fort Collins, CO.

Banks, D., and Meroney, R. N. (2001a). "The Applicability of Quasi-Steady Theory to Pressure Statistics Beneath Roof-Top Vortices." *Journal of Wind Engineering and Industrial Aerodynamics*, 89(6), 569-598.

Banks, D., and Meroney, R. N. (2001b). "A Model of Roof-Top Surface Pressures Produced by Conical Vortices: Model Development." *Wind and Structures*, 4(3).

Banks, D., and Meroney, R. N. (2002). "A Model of Roof-Top Surface Pressures Produced by Conical Vortices: Evaluation and Implications." *Wind and Structures*, 5(1).

Banks, D., Meroney, R. N., Sarkar, P. P., Zhao, Z., and Wu, F. (2000). "Flow visualization of conical vortices on flat roofs with simultaneous surface pressure measurement." *Journal of Wind Engineering and Industrial Aerodynamics*, 84(1), 65-85.

Bienkiewicz, B., and Sun, Y. (1992). "Local Wind Loading on the Roof of a Low-Rise Building." *Journal of Wind Engineering and Industrial Aerodynamics*, 45, 11-24.

Cermak, J. E. "Wind Damage Mitigation - Wind engineering challenges." *International Conference on Wind Effects on Buildings and Structures*, Porto Alegre, Brazil.

Cochran, L. S., and English, E. (1997). "Reduction of Roof Wind Loads by Architectural Features." *Architectural Science Review*, 40, 79-87.

FEMA. (1992). "Building Performance: Hurricane Andrew in Florida." , Federal Emergency Management Agency, Washington DC.

Ham, H. J., and Bienkiewicz, B. (1998). "Wind tunnel simulation of TTU flow and building roof pressure." *Journal of Wind Engineering and Industrial Aerodynamics*, 77 & 78, 119-133.

Kramer, C., and Haage, K. (1975). "Suction Reduction Installation for Roofs." , United States.

Levitan, M. L., and Mehta, K. C. (1992). "Texas Tech field experiments for wind loads part 1: building and pressure measuring system." *Journal of Wind Engineering and Industrial Aerodynamics*, 41-44, 1565-1576.

National Research Council (1985). "Hurricanes Iwa, Alicia, and Diana -- Common Themes.", National Research Council Committee on Natural Disasters, Washington, DC.

Lin, J. X., and Surry, D. "Suppressing extreme suction on low buildings by modifying the roof corner geometry." *7th US National Conference on Wind Engineering*, Los Angeles, 413-422.

Richardson, G. M., and Surry, D. (1994). "The Silsoe Structures Building: Comparison between full-scale and wind-tunnel data." *Journal of Wind Engineering and Industrial Aerodynamics*, 51, 157-176.

Saathoff, P. J., and Melbourne, W. H. (1989). "The generation of peak pressures in separated/ reattaching flows." *Journal of Wind Engineering and Industrial Aerodynamics*, 32, 121-134.

Surry, D., and Lin, J. X. (1995). "The effect of surroundings and roof corner geometric modifications on roof pressures on low-rise buildings." *J. Wind Eng. Ind. Aerodyn*, 58, 113-138.

Wu, F. (2000). "Full-Scale Study of Conical Vortices and Their Effects Near Roof Corners," Ph.D., Texas Tech University, Lubbock.

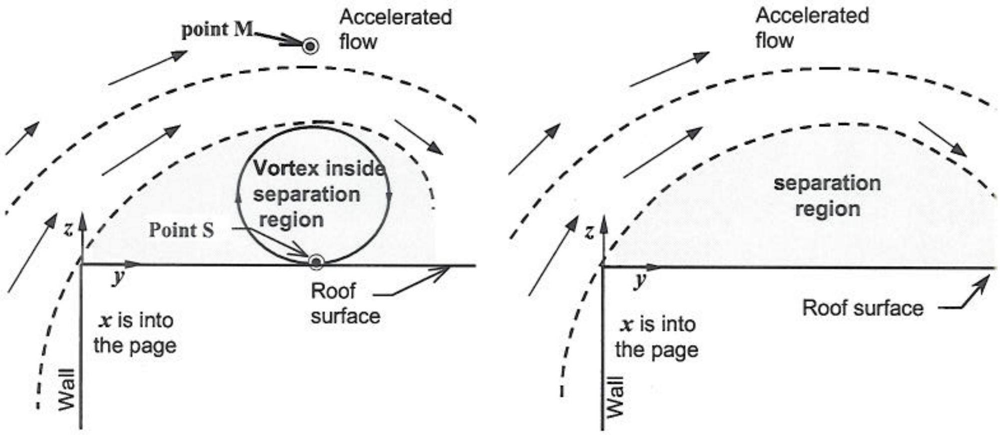

Figure 1: Separated flow region behind leading edge of roof.

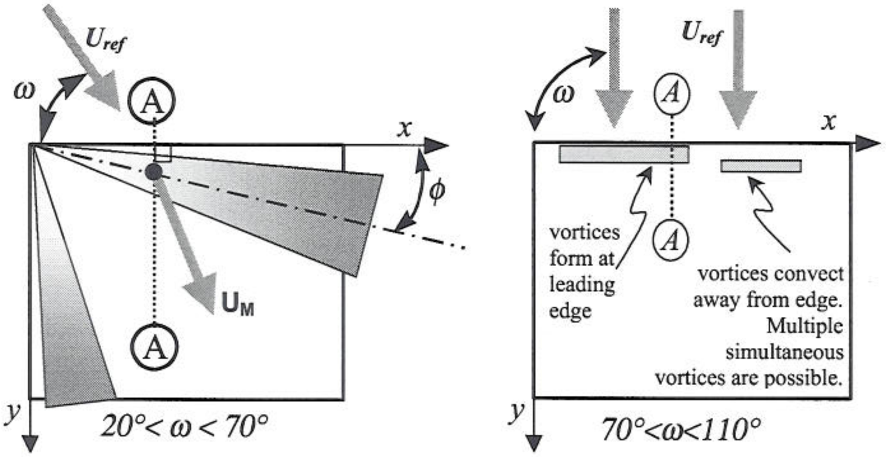

Figure 2: Top view of roof, showing conical vortices (left) and cylindrical vortex in bubble separation (right). Note that Figure 1 presents side view through the lines A-A.

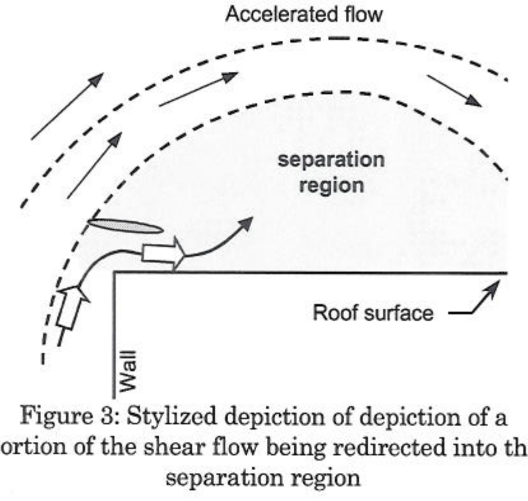

Figure 3: Stylized depiction of depiction of a portion of the shear flow being redirected into the separation region

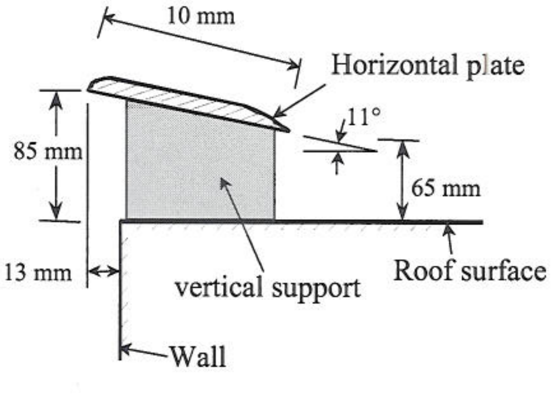

Figure 4: Dimensions of the prototype flow divider device tested on the TTU WERFL building

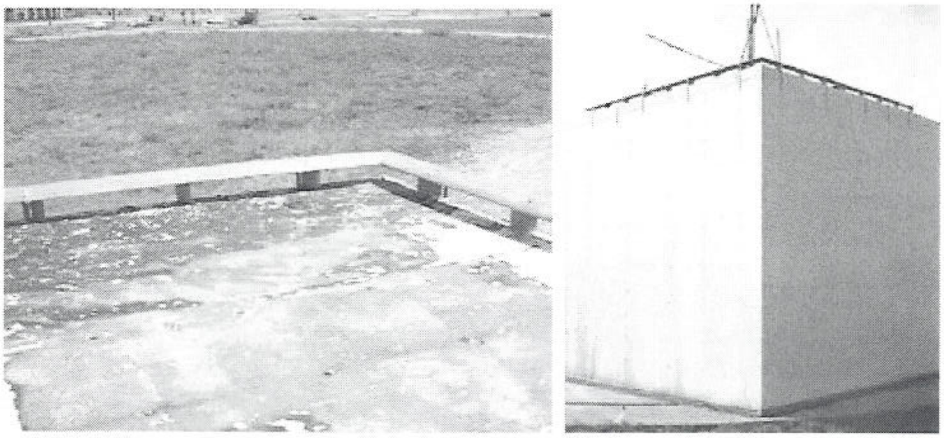

Figure 5: Photographs of the prototype flow divider as tested on the TTU WERFL building.

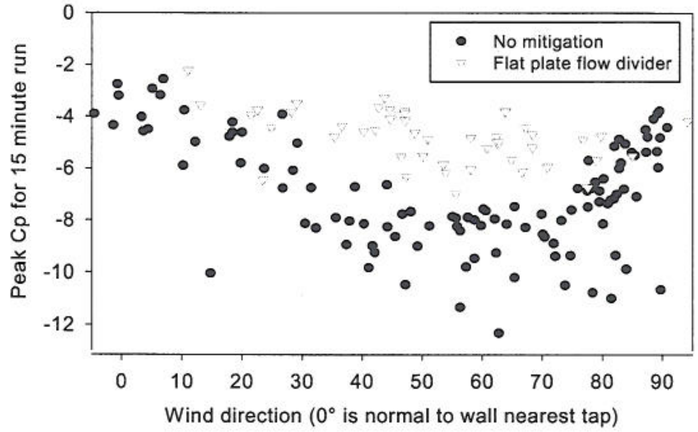

Figure 6: Reduction in peak suction at tap 50501 due to flow dividing mitigation device (full scale tests).

tap#	x (mm)	y (mm)
	“2ft.” row	
2	18.5	5.6
3	18.5	11.1
4	18.5	18.6
	“3 ft” row	
7	31.6	8.6
8	31.2	14
9	31.5	21
10	31.5	26.7
	“4 ft” row	
11	44.8	8.5
12	44	14
13	44.5	20.2
14	45	26.6
15	44.6	32.6
16	44.6	38.6
17	45	44.6

“5 ft” row

tap#	x (mm)	y (mm)
18	56.5	8.4
19	56.6	14.2
20	57	20
21	56.6	26.8
22	57	32.7
23	57	38.8
24	56.6	45.5
25	56.3	56.2
26	54.5	63
27	59	112

“9 ft” row

tap#	x (mm)	y (mm)
28	106	14.5
29	106.1	19.9
30	106.5	27
31	107	33
32	106.4	39.7
33	106	51.1
34	106.5	63.5
35	106.5	85.8
36	107	112

other taps

1	12.1	14.6	41	258.5	28
37	183.5	126	42	258.5	126.5
38	183.5	226	43	12.4	272
39	183.5	324.5	44	85.3	272
40	183.5	424	45	282.7	272

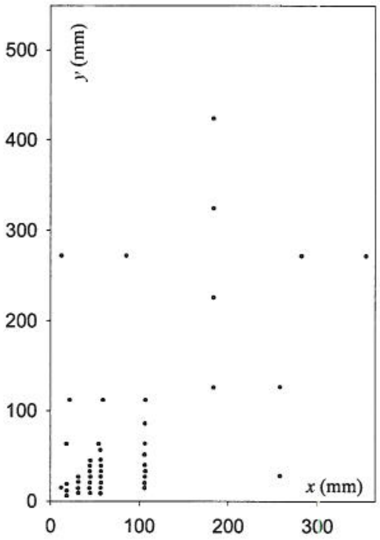

Figure 7: Tap locations on 1:25 TTU WERFL building model roof. Taps 1-3, 5, 6, 11-14, 18-23, 26-34, & 36 correspond to taps installed on the full-scale site.

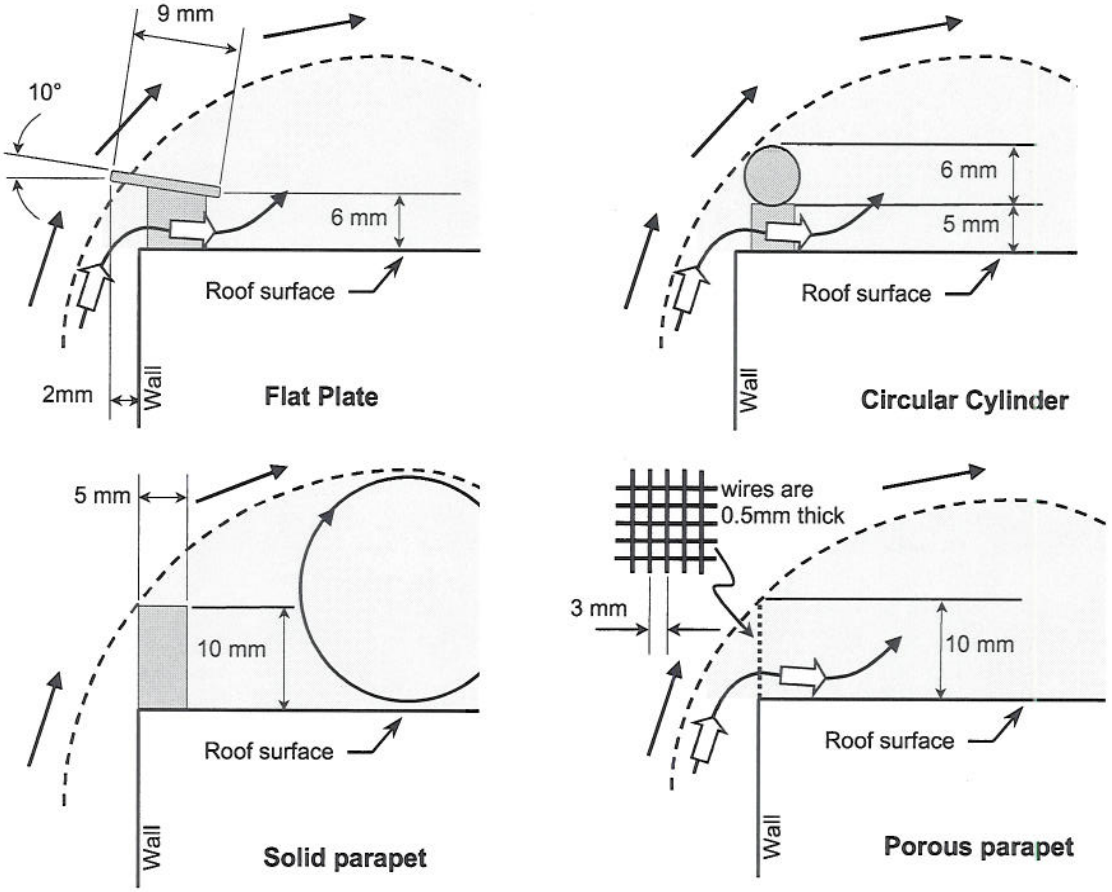

Figure 8: Roof edge devices tested in the wind tunnel (model scale dimensions)

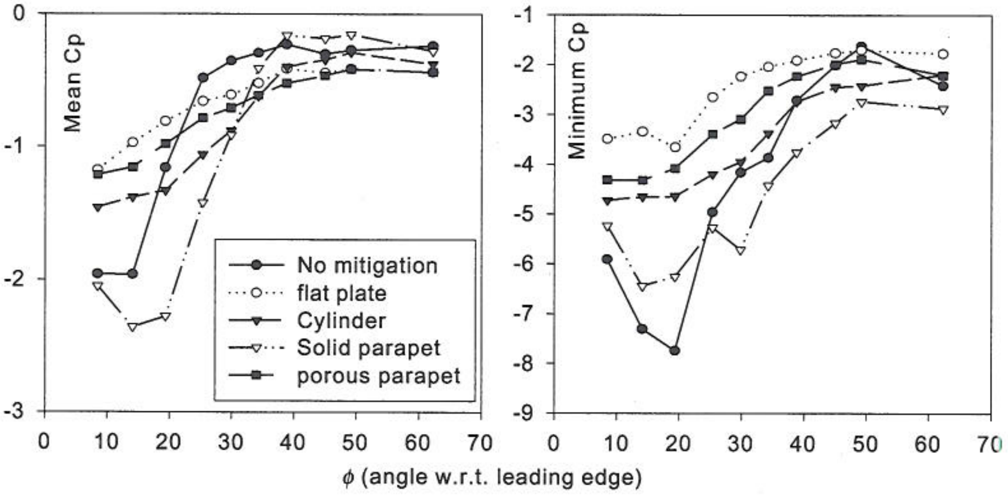

Figure 9: Roof-top pressure coefficients with and without mitigation measures for $\omega = 50°$, for a row of taps at 1.44m (nominally 5 ft) from the corner. ϕ is defined in Figure 2.

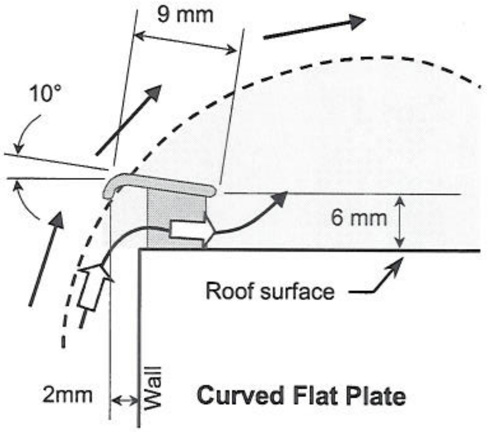

Figure 10a Curve plate divider

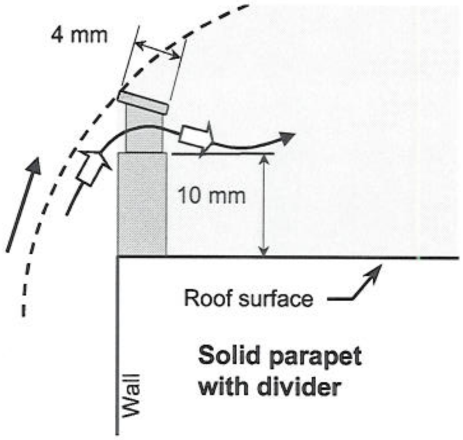

Figure 10b: Divider on Solid Parapet

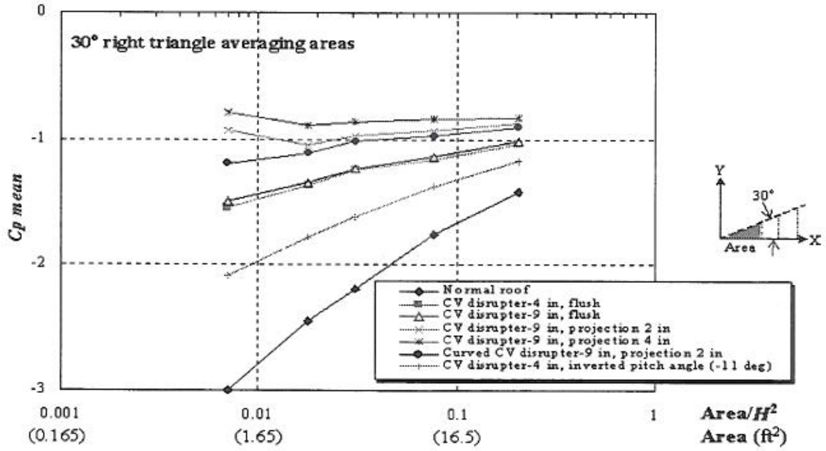

(a) Mean area-averaged pressure coefficients.

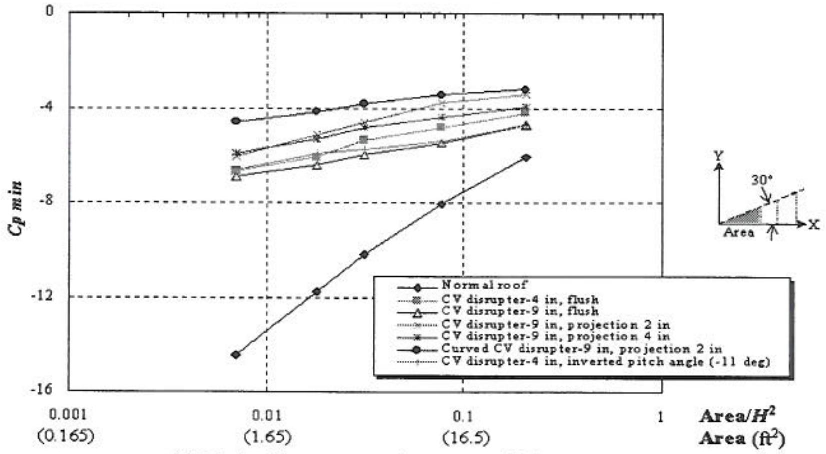

(b) Min (peak) area-averaged pressure coefficients.

Figure 11: Effect of various flat plate flow deflecting devices (here referred to as the "conical vortex disrupter") on area averaged wind loads for triangular roof edge region. Tests done with $\omega = 50°$.

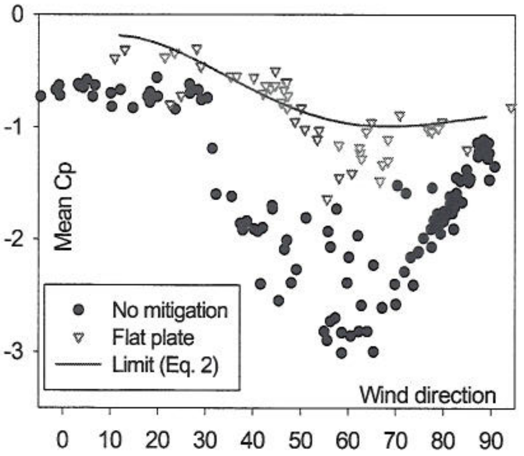

Figure 12a: Full scale data for tap 50501.
UM data for limit measured in wind tunnel

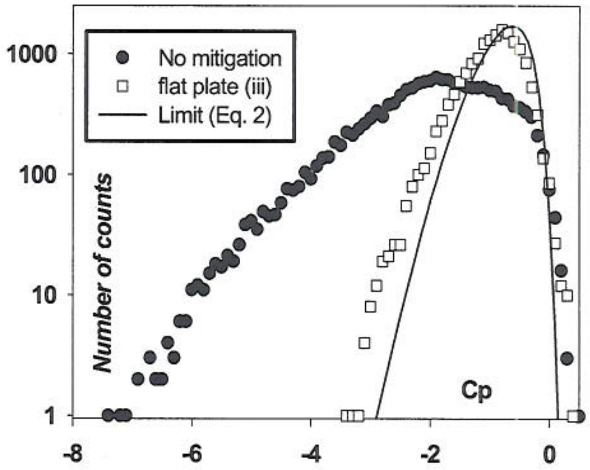

Figure 12b: Cp PDF for tap #12.
All data from wind tunnel measurements.

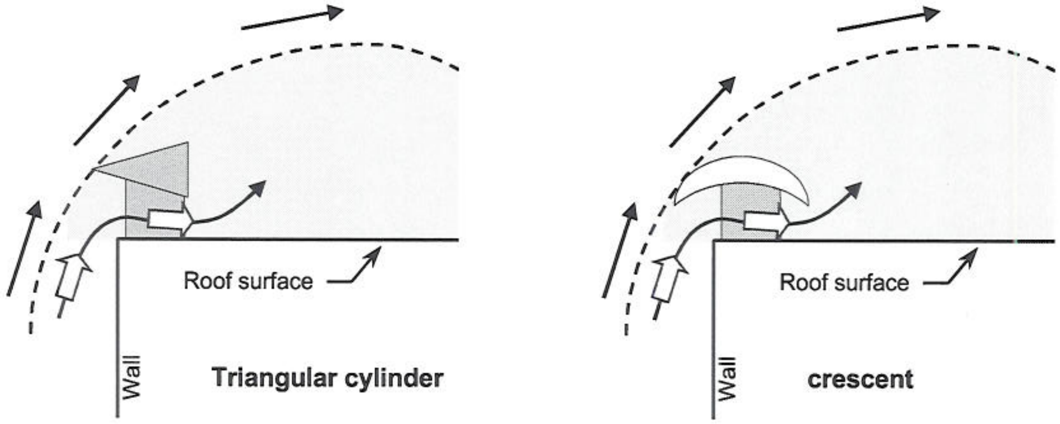

Figure 13: Alternative flow divider shapes and configurations

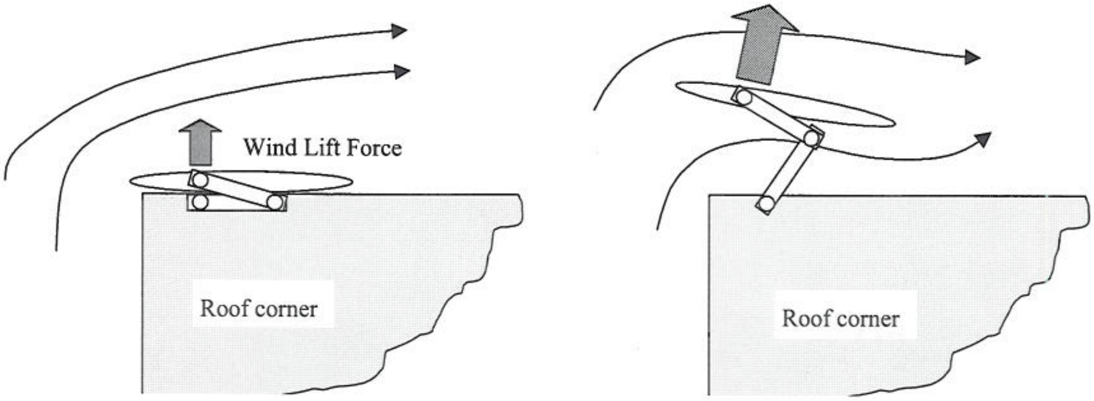

Figure14: Wind uplift can be used to deploy the mitigation device.